Quantification of particle number concentration in liposomal suspensions by Laser Transmission Spectroscopy (LTS)

Simona Sennato [a,b,*,1,2], Angelo Sarra [a,c,1], Carlo Panella La Capria [b], Cecilia Bombelli [d], Enrica Donati [e], Paolo Postorino [b], Federico Bordi [a,b]

[a] *Institute for Complex Systems, National Research Council (CNR-ISC), Sapienza University of Rome, Piazzale Aldo Moro 2, 00185, Rome, Italy*
[b] *Physics Department, Sapienza University of Rome, Piazzale Aldo Moro 2, 00185, Rome, Italy*
[c] *Microscopy Center, University of L'Aquila, Via Vetoio, Coppito, L' Aquila 67100, Italy*
[d] *Institute for Biological Systems, National Research Council (ISB-CNR) Secondary Office of Rome-Reaction Mechanisms c/o Department of Chemistry, Sapienza University of Rome, P.le A. Moro 5, 00185 Rome, Italy*
[e] *Institute for Biological Systems, National Research Council (ISB-CNR), Rome1 Research Area, Strada Provinciale 35d 9, Montelibretti, Rome 00010, Italy*

ARTICLE INFO

ABSTRACT

Laser Transmission Spectroscopy (LTS) is an experimental technique able to determine the particle number concentration and the size of colloidal suspensions by a single measurement of the transmittance of a laser beam through the suspension of particles as a function of the wavelength. In this protocol, we show that LTS represents a unique and powerful tool to investigate suspensions of liposomes, where the precise quantification of the number concentration is particularly relevant for the complete definition of the colloidal properties of the suspension. We study a model formulation of Soy-PC:Chol liposomes and we validate LTS results by comparison with High-Performance Liquid Chromatography determination of lipid mass. Then LTS protocols is applied to state-of-art liposomal nanocarrier suspensions. We explain details of data analysis to obtain the particle number concentration by using the Lambert-Beer law and by calculating the extinction cross section, within the framework of Mie theory for spherical vesicles. We also determine the liposome radius and compare it with the hydrodynamic radius measured by Dynamic Light Scattering. As future perspective, we aim to extend LTS analysis to other nanostructures with different geometries and to contribute to the development of new quantitative strategies for the accurate characterization of nanocarriers and other nanoparticles.

1. Introduction

The precise determination and control of the number concentration of a drug nanocarrier is a crucial point in nanomedicine to maximize the drug efficacy and minimize its toxicity for *in vivo* administration [1]. Large uncertainties on this parameter can lead to unreliable or wrong conclusions in comparative toxicity and other *in vitro* assays. As a matter of fact, exposure of cells to different number of particles could imply different uptake activities, endo/phagocytosis events, or other confusing phenomena [2]. For this reason, FDA draft guidance on nanocarriers formulations suggests to report the particle number concentration in addition to the commonly used particle mean size and polidispersity [3].

Since the number- and mass-based size distributions calculated by Dynamic Light Scattering (DLS) are affected by large unavoidable errors [4], there is a particularly strong need for reliable methods [3].

Several strategies are under development to overcome this major challenge in nanoparticle characterization [5]. Available techniques include the measurement of ensemble physical properties of nanoparticle dispersions (e.g., light absorption or scattering), or the direct counting of individual particles by optical microscopy or sensors.

UV–Vis absorbance is able to supply a reliable value of the number concentration for metallic and semiconductor nanoparticles if their molar extinction coefficient is known [6]. For non-adsorbing particles, UV-based turbidimetry can give results in good agreement with

---

estimates from weight only for monodisperse systems with a known refractive index and scattering coefficient, such as latex or silica particles, moreover its sensitivity decreases with size [5]. Conversely, for non-monodisperse suspensions as polymeric nanocarriers and drug-loaded liposomes, the variation of size and drug content affects turbidity, which also depends on their internal structure [7]. Similarly, the possibility of obtaining the particle number concentration by DLS photon count rate is restricted to monodisperse samples and in the presence of a calibration with a standard sample of the same size, optical properties, and dispersing solvent [8]. Counting individual nanoparticles under direct visualization can provide the particle number concentration without the need of standards, although a high statistics is hard to obtain. Transmission Electron Microscopy (TEM) has long been considered as the best suited for its resolution up to the nanometric range, but it is prone to artifacts and limitations for soft organic samples with low electron density. First, it requires staining molecules to increase the contrast. More, particle identification becomes complex when samples undergo deformation and aggregation during drying process. Among non-microscopy-based counting techniques, Tunable Resistive Pulse Sensing (TRPS) is able to relate the number of particles to the detected changes in current or resistance when particles pass through an electric field [9]. Recent instruments allow the detection of particles of any nature with sizes from 10 μm to 50 nm, further reduced up to 10 nm thanks to the advancements in nanopore technology [10]. The major limitation of this method lies in the necessity of a standard nanoparticle sample with known concentration to calibrate the pulse count.

The recent integration of counting with light scattering and optical detection techniques enabled the development of the Nanoparticle Tracking Analysis (NTA) platforms which can give concentration values close to the real ones for monodisperse systems with size larger than 40–50 nm and strong scattering capability. Unfortunately, limitation in colloidal polydispersity represents a major drawback, due to an overestimation of the number of larger particles. The particle refractive index and the signal-to-noise ratio, which decreases as nanoparticle size decreases, further restrict the minimal detectable size. The smallest reliable diameter for liposomes is around ∼ 40 nm. Background signals originated from instrument fluctuations and impurities can impact the concentration values substantially.

In last few years, different research groups implemented setups based on a new optical technique referred to as "Laser Transmission Spectroscopy" (LTS) able to get the particle number concentration and their geometrical size by a single measurement of the wavelength-dependent transmission coefficient of the suspension [11–14]. By changing the laser light source with a deuterium-tungsten lamp and using a spectrometer as the detector, a real-time instrument for measurement of aerosol was also built [15]. LTS results appeared very promising, especially in terms of sensitivity, which is several order of magnitude higher than DLS for polystyrene particles in the size range 50–3000 nm.

In a suspension of identical spherical particles with radius r, the relation between the particle number density distribution $n(r)$ and the transmitted intensity for a determined wavelength $T(\lambda_i)$ is given by the Beer-Lambert's law

$$T(\lambda_i) = \exp^{-\sigma_{ext}(\lambda_i, r)n(r)z} \tag{1}$$

where z is the optical path within the sample and σ_{ext} is the extinction cross-section. For particles of different sizes, $T(\lambda_i)$ becomes the product of the transmittance for each "class" of particles grouped by different radius r_j and density n_j

$$T(\lambda_i) = \prod_{j=1}^{N} T(\lambda_i, r_j) = \exp^{\sum_{j=1}^{N} -\sigma_{ext}(\lambda_i, r_j)n_j z} \tag{2}$$

thus the extinction coefficient $\alpha_{ext}(\lambda_i)$ is defined as

$$\alpha_{ext}(\lambda_i) = -\frac{\ln(T(\lambda_i))}{z} = \sum_{J=1}^{N} -\sigma_{ext}(\lambda_i, r_j)n_j \tag{3}$$

Therefore, for a single LTS measurement a set of equations (3) is obtained, each one for a measured wavelength. This set of equations would allow in principle to calculate the particle number concentration n_j as a function of each size r_j. However, due to the presence of experimental uncertainties (noise) a numerical approach is necessary and data analysis requires special attention. In particular, the theoretical values of the extinction cross section $\sigma_{ext}(\lambda_i, r_j)$ can be computed through the Mie scattering theory for spheres (or Adan-Kerker for shelled spheres) [6, 16]. Then, using the Tikhonov regularized square-root based algorithm [17], it is possible to solve the equation system to obtain the particle number density distribution $n_j(r_j)$. Note that the sum over the whole set of r_j of this distribution gives the total particle number concentration of the analyzed sample.

Since LTS technique adopts a general and simple approach based on Mie scattering, it can overcome the limitation of range of particle size and the need of a calibration standard, adding the advantage of the large statistical significance typical of a bulk technique. Moreover, it allows to determine the size of the particles in suspension by means of the same measurement and it can be of valuable help in inferring useful information on the shape and structure of the particles (for example the presence of coatings or shells surrounding the particles), thus responding to the necessity to develop a universal methodology compatible with objects of different size, nature and geometry. The simultaneous determination of the geometrical size and particle number offers the advantage to improve the accuracy of the calculation of the colloidal volume fraction ϕ, i.e. the fraction of the total volume V that is filled by n spheres, each of radius r, $\Phi = 4/3\pi r^3 n/V$. This parameter is relevant for understanding the behaviour of the "hard spheres" model system well known in soft condensed matter science. Its accurate experimental determination allows a more reliable comparison between experiments and theories and simulations [18]. Moreover, while here we limit ourselves to consider only coated spherical particles, the LTS technique can be in principle adapted to characterize nanoparticles of different shape and geometry (for example cylinders, disks, ellipses, etc.) using the proper algorithms to calculate numerically the extinction coefficients in the framework of the scattering theory. This offers the opportunity to extend the application of the LTS method to nanocarriers of different nature as well as to tackle the problem of the determination of volume fraction in non-hard sphere colloidal systems, such as polymeric micelles or star polymers, which have a wide fundamental and applicative interest as nanocarrier systems. Note that the knowledge of the volume fraction in a nanocarrier suspension allows to calculate the total volume available for drug encapsulation and analyse the drug loading capability on a complementary point of view to the commonly used definition of drug loading efficiency [19].

We have recently explored the LTS application to the investigation of natural and synthetic lipid vesicles, as exosomes and liposomes [14, 19–21]. In this protocol paper, we explain the use of our LTS set-up to determine the particle number concentration of liposomes by examining model and state-of-art formulations in the typical concentration range used to investigate these systems. We examine a model formulation of SoyPC:Chol liposomes and validate LTS results by comparison with High-Performance Liquid Chromatography (HPLC) determination of lipid mass, then we apply LTS protocol to novel liposomal nanocarriers. We show how number concentration can be obtained by data analysis by the Lambert-Beer law and calculation of the extinction cross section, in the framework of Mie theory for spherical vesicles. Liposomal vesicles represent the most common type of nano-drugs approved by FDA. Particle number, rather than merely their size, affects the effective uptake by specific cells such as phagocytic cells, and the cumulative drug content of the particles/carrier determines their bioactivity [22].

Here we provide the theoretical and all the technical details on the

LTS measurement procedure and data analysis of liposomal suspensions. Our results demonstrate that the proposed methodology is a powerful, reliable tool for research in colloidal science and chemistry as well and it is valuable for a deep drug nanocarrier characterization.

2. Materials and preparatory procedures applied

2.1. Preparation of liposomal suspensions

Prepare liposomal suspensions using the reagents listed in Table 1 according to the film hydration method [23] coupled with the freeze-thaw protocol and extrusion [24].

1. Prepare lipid solutions in volumetric flasks by adding to the weighted powder $CHCl_3$ or, in the case of DPPG, a $CHCl_3/MeOH/H_2O$ 2:1:0.15 mixture. Then, add the proper amounts of each solution in a round-bottom flask, in order to obtain the desired molar ratio of the lipid components. By gentle removing of the organic solvent by rotary evaporator, you will obtain a thin lipid film of lipids on the wall of the round-bottom flask. After storage under reduced pressure for at least 6 hours, add Hepes buffer containing or not the hydrophilic drug (Isoniazid, INH), and vortex-mix the solution to obtain the lipid dispersion of multilamellar vesicles (MLVs). **Crucial step** During vortex-mixing process, check the complete detachment of the lipid film from the flask wall to avoid lipid loss.
2. Freeze-thaw the dispersion from liquid nitrogen to 313 K to reduce the lamellarity of the aggregates. For encapsulation of small hydrophilic molecules as INH, this procedure helps in increasing the drug encapsulation efficiency [25]. **Crucial step**. Pay attention from one hand to freeze completely the sample in liquid nitrogen and, from the other, to warm it sufficiently to go beyond the lipid transition temperature. A carefully execution of this step will allow a real reduction of MLV and a faster extrusion.
3. Extrude the dispersion (10 times) through a 100 nm polycarbonate membrane to obtain unilamellar vesicles. Perform the extrusion at a temperature well above the transition temperature of the used lipids.
4. For INH-loaded liposomes, eliminate the excess drug in the solution by purification in spin columns (see SI for details).

2.2. Setup of the LTS apparatus

The scheme of our LTS setup is shown in Fig. 1 and the equipment is listed in Table 2. The laser system employs a pulsed Nd:YAG source, with 5 ns pulse duration and 10 Hz repetition rate. The laser tunability in the wavelength range 410–2600 nm (extendable down to 210 nm) is obtained through a non-linear optic system that employs crystals for the generation of second and third harmonic and an optical parametric

Table 1
List of materials and reagents. [Mw: molecular weight].

Materials and reagents	Manufacturer	City and Country
Soybean Phosphatidylcholine S-100 (Soy-PC) [Mw 776]		
Hydrogenated Soybean Phosphatidylcholine E PC3 (HSPC) [Mw 762.1]	Lipoid GmbH	Ludwigshafen am Rhein, Germany
Dipalmitoyl-Phosphatidyl-glycerol, sodium salt (DPPG-Na) [Mw 745]		
Cholesterol (Chol) [Mw 386.6]		
Isoniazid (INH) [Mw 737]	Sigma-Aldrich	Zwijndrecht, The Netherlands
4-(2-hydroxyethyl)− 1-piperazine ethanesulfonic acid (Hepes)		
Methanol (MeOH), Chloroform ($CHCl_3$), Acetonitrile (ACN) (HPLC grade)	VWR International S.r.l.	Milan, Italy
MilliQ-grade water	Sartorius	Milan, Italy

oscillator. The beam intensity is attenuated by a set of neutral density filters (ND) to avoid optic and sample damages, which may occur in the presence of degradable components, such as organic molecules and dyes. A set of broadband reflecting mirrors (M) allows to align the laser beam parallel to the surface of the optical table and to direct it on a broadband polka-dot 50/50 beam splitter (BS), that equally divides the laser beam onto two optical paths. The laser beam passes through the cuvettes (C) (hosted in a temperature controlled Peltier system) containing the sample (S) and the reference (R), then it reaches two Si photodiodes (PDS, PDR) that measure the variations of the transmitted laser intensities and generate proportional voltage responses. These PDS and PDR generated voltages are the input signals of an homemade lock-in amplifier (LIA) whose outputs are digitized and sent to a PC for the measurement acquisition in a LabVIEW environment.

3. Methods according to the protocol

3.1. LTS measurements of liposomal dispersion

The LTS apparatus (Fig. 1) allows the simultaneous measurement of light intensity transmitted by the sample (S) of particles with radius r, and on the medium in which the particles are suspended (the reference, R), giving a set of discrete values of the measured voltages at each λ_i, $S(\lambda_i, r)$ and $R(\lambda_i)$, respectively. The transmission coefficient $T(\lambda_i, r)$ of the particle can be calculated as

$$T(\lambda_i, r) = \frac{S(\lambda_i, r)}{R(\lambda_i)} \qquad (4)$$

The light intensity impinging on the photodiodes contains also spurious wavelength-dependent contributions related to the specified optical path (that account for all optics wavelength transmission variations), to the detector sensitivities and to the gains of the LIA channels [11,14]. It is necessary to cancel them out to avoid alteration of the results. Li et al. [11] showed that the detector signals S and R can be written as the product of different quantities, i.e. the power of the laser beam of the specific channel, the efficiency of the detector and the transmittance of the particles and of the medium. They proposed the so-called "double ratio" method, consisting in repeating the measurement twice exchanging S and R in the two optical paths A and B, so to obtain two distinct ratios S/R (hence the name "double ratio") which can be combined together so that only the transmission coefficient of the particles remains.

Recently some of us proposed a new approach to LTS measurements called "variable gain calibration procedure", that makes use of an ad-hoc designed tunable-gain, dual-channel, dual-phase LIA suitably designed and optimized in terms of the detection sensitivity and resolution [14]. With respect to the standard "double-ratio" method, this method makes use of a single calibration procedure to balance the signals coming from the S and R channels when in both the channels is present the suspending medium only. This balanced LTS method is performed by suitably varying the gain of the two LIA channels so to achieve the same value of the S and R signals for each wavelength of the laser beam. The values of the wavelength dependent gains determined by this calibration procedure are then used for the LTS measurement of the particles under investigation located in the sample channel. This "variable gain procedure" allow to decrease of an order of magnitude the experimental indetermination of the particle size respect to the double ratio technique [14].

For the investigation of liposomal suspensions, we report the following procedure:

1. Clean two identical (same batch) quartz cuvettes and dry them with Nitrogen flux. **Crucial step** Any contaminant should be removed to avoid interference. Clean also the external optical surface by optical paper.
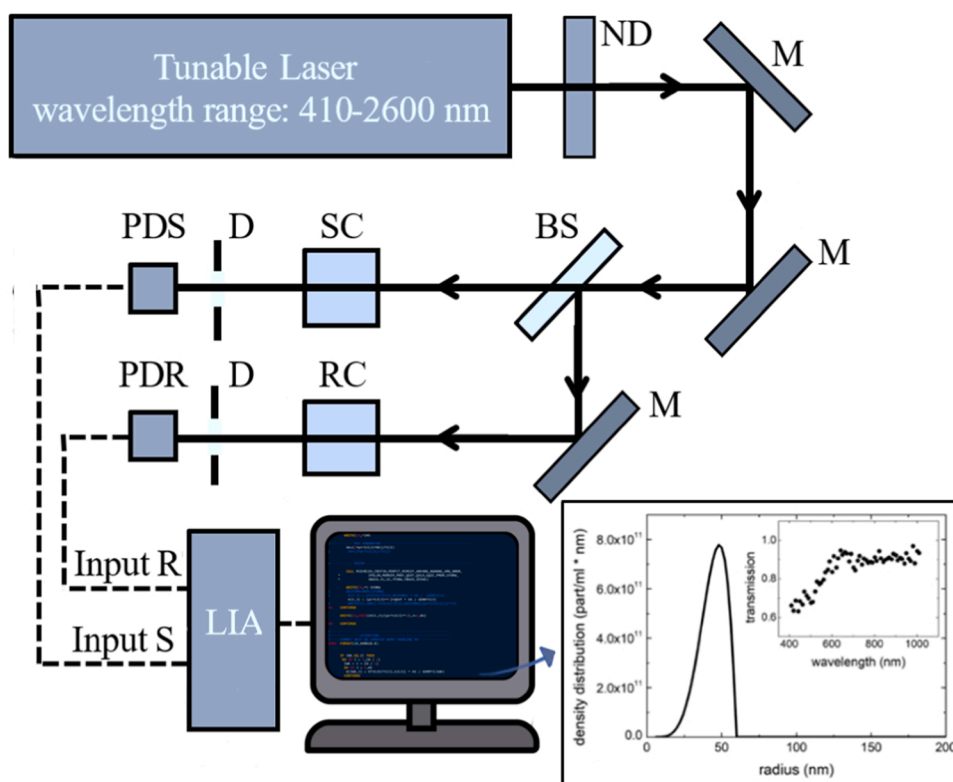
Fig. 1. Scheme of the LTS apparatus and its optical components: neutral density filters (ND), broadband fully reflecting mirrors (M), broadband 50/50 beamsplitter (BS), sample and reference cuvettes (SC, RC), diaphragms (D) and Si photodiodes (PDS, PDR). Si photodiodes output two voltages proportional to the light intensity passing the sample and reference, that are amplified by a Lock-In Amplifier (LIA) and acquired through a data acquisition board by a PC. After the computation of the extinction coefficient and analysis through LTS Fortran program, it provides the particles density distribution of the sample.

Table 2
Equipment composing LTS set-up. Abbreviations are indicated in the brackets.

Component	Manufacturer	City and Country
5 ns Q-Switched Nd:YAG NT342B laser	Ekspla	Vilnius - LT
Polka-Dot Beam Splitter (BS)	Edmund Optics	US
Deep Ultra Violet Enhanced type mirror (M)	Edmund Optics	US
DET10A2 Si Photodiodes (PDS, PDR)	Thorlabs	US
dual phase Lock-In Amplifier (LIA)	University of L'Aquila	Italy
quartz cuvettes (C)	Hellma	Germany
LTS User-Interface Lab view acquisition software	home-made	Rome, Italy

2. Switch on the laser source by the controlling software. **Crucial step** A shutter is placed to close the laser opening to protect users from exposition. Check the positioning of the ND filters (choose the appropriate optical density) to attenuate the beam intensity to avoid sample and optics damage besides saturation of detectors. Note that the configuration of ND filters has to be changed to get the best one with respect to the measured wavelength range sub-interval.

3. Use a thermostated sample holder and adjust the temperature setting. The measurements of this protocol have been carried out at 20°C.

4. Fill S and R cuvettes with 1 ml of liposomal sample and of the aqueous medium, respectively. Place them into the thermostated sample holder and take note of their position. **Crucial step** Make sure that incident beams cross the cuvettes inside the filled volume and no reflection at the air-water interface occurs.

5. A set of measurement parameters must be chosen to define the wavelength interval, the lasering time for each wavelength and the acquisition time for each wavelength (taking into account the LIA integration time). For our setup, through the Labview home-made

"LTS-User Interface" (LTS-UI), it is possible to set the following parameters:
– Min wavelength (minimum of range)
– Max wavelength (maximum of range)
– Exposure time (overall lasering time for each wavelength)
– Time delay (time delay before sampling the LIA signal)
– Number of sampling points (to obtain average values of the voltage)

Crucial step The wavelength interval of acquisition must be defined in order to observe the majority of the 0–1 $T(\lambda, r)$ dynamic range. For colloids with diameter ranging from $30 \div 300$ nm and concentration $10^8 \div 10^{11}$ part/ml, this wavelength interval is approximately $210 \div 800$ nm. To help in setting the acquisition interval, it is useful to simulate the expected transmission coefficient from a shelled sphere by freely-available Mie theory calculators. Time delay represents the integration time of LIA and its value has to be chosen considering the LIA time constant [14]. Here it was fixed to 10 seconds. Fix the number of sampling points in order to have a good compromise between statistical significance of average values and overall measurement time duration. Usually we used 30 points, considering a fixed sampling frequency of 1 Hz). Then the exposure time must be the sum of time delay and of the resulting sampling time (e.g. 30 points * 1 Hz = 30 s).

6. Start the measurement with the optimised configuration and acquire the data in the chosen wavelength range.

3.2. Analysis of extinction coefficient of liposomal dispersion within the Mie theory

The equation (3) connects in a simple way the measured transmission coefficient as a function of wavelength $T(\lambda_i)$ with the density of particles n_j of radius r_j. Note that it represents a system of linear equations with unknowns n_j, obtained by setting the measured extinction coefficients at each wavelength equal to the theoretical extinction

coefficients. Therefore, as introduced before, to obtain the density distribution of particles as a function of size n_j, we have to:

1. calculate the theoretical extinction matrix $\sigma_{ext}(\lambda_i, r_j)$;
2. invert the equations system $\alpha_{ext} = \sum_{j=1}^{N} \sigma_{ext}(\lambda_i, r_j) n_j$.

This represents a typical "ill-posed" problem known as Fredholm integral equation, whose solution typically needs a least-squares minimization algorithm [26,27]. It is well known that this approach may lead to multiple solutions, most of which are non-physical. A regularization term is introduced to filter out the non-physical solutions. We use the most common method called Tikhonov regularization where a regularization parameter Λ, and the matrix with elements δ_{ij} are used to impose restrictions that give preference to non-oscillatory solutions, which are calculated by minimizing the sum of the squares of the deviations along with the regularization term

$$\| \sigma_{ij} n_j - \alpha_i \|^2 + \| \Lambda \, \delta_{ij} \cdot n_j \|^2 \tag{5}$$

To perform these calculation we use the subroutines available in literature for the extinction matrix calculation, i.e. BHCOAT.f for shelled spheres [6], and the freely available FORTRAN program FTIKREG.f, that inverts the linear equation system using the Tikhonov regularization [17,28,29]. These routine have been combined in a home-built analysis software based on a FORTRAN code (LTS.f).

The calculation of the extinction matrix (via BHCOAT.f) needs the knowledge of wavelength-dependent indexes of refraction of shell, core and suspending medium. In the LTS.f code we included a series of Sellmeier's equations of different materials (polystyrene, cellulose, water, etc.) [30–33], that can be chosen as refractive index model. This allows to obtain a LTS program for each shelled structure, with a particular core and a defined suspending medium. Each of this LTS.f program is structured as the flow chart reported in Fig. 2, where the

blocks relative to the main program FTIKREG.f and the subroutines BHCOAT.f are highlighted with different colors.

LTS.f reads the measured extinction coefficient α_i and the associated experimental error $\Delta\alpha_i$ for each wavelength λ_i, saved as an input data in an ASCII file named LTS.dat. After the computation, the program writes the estimated solution (number of particles n_j and the estimate bin error Δn_j for each radius r_j) in a output ASCII file called LTS.sol. Check that input LTS.dat file contains only three numerical columns, because whichever non-numeric value cannot be read by the program. A third ASCII file (LTS.par) contains the parameters that govern FTIKREG.f. This file contains two columns, the first with the numerical values and the second with the name of the parameters, whose meaning is explained below.

- *ns*: number of points used to calculate the density distribution $n(r)$ ($2 \leq ns \leq 7000$);
- *smin*: minimum radius at which the density distribution $n(r)$ should be calculated;
- *smax*: maximum radius at which the density distribution $n(r)$ should be calculated;
- *n*: total number of data points (the same number of measured $\alpha(\lambda)$ in LTS.dat);
- *errmod*: type of data errors used for calculation. The parameter has two digits. The first digit determines if the error must be multiplied by a scaling factor defined by the parameter error (digit value equal to 1) or by a scaling factor calculated by the program (equal to 2). The second digit determines if the data errors (multiplied by the scaling factor) are read from LTS.dat (digit value equal to 1) or the data are assumed with an absolute error (equal to 2) or relative error (equal to 3);
- *error*: error scaling factor. This value is used only if the first digit of *errmod* is equal to 1. For *errmod* = 12 or *errmod* = 13, this parameter is an estimation of the absolute or relative error, respectively.

For the extinction coefficient analysis with LTS software, we report the following procedure: .

1. Copy the wavelengths, the measured extinction values and the experimental errors into LTS.dat file, in three distinct columns. **Crucial step** Check the presence of any text spacing in the three columns, that would cause reading error. Beyond this, ensure that values in exponential notation are written according this notation 1,87E-12 (or 1,87D-12 if double precision is used).
2. Set the parameters outlined above in LTS.par file. **Crucial step** For a good analysis response, set *ns*, *smin* and *smax* to have a spacing of reconstructed radii close to the measured wavelength spacing (e.g. for a wavelength collected with 10 nm step, use *ns* = 100, *smin* = 1, *smax* = 1001). A fundamental choice is for error parameter because it governs the contribution of experimental error of α_{ext}, that, as known, introduces possible multiple solutions of the system. If *errmod* is set to 11, the parameter error must be close to 1, with small variation permitted around this value. Indeed, it represents a scaling factor of experimental error in LTS.dat and can be changed to overcome possible convergence problems of the algorithm.
3. Analyse the particle density distribution obtained in LTS.sol file. Note that the third column is the error of each bin of the distribution and represents an estimation of the quality of distribution itself. **Crucial step** The mean radius is calculated as the weighted average on the distribution and so it is a number weighted radius. The total particle number concentration is obtained as the area under the curve, i.e. the integral of the distribution. When the particle density distribution shows two distinct populations (bimodal distribution), the ratio between the area calculated on each distribution gives the number ratio between the two populations.
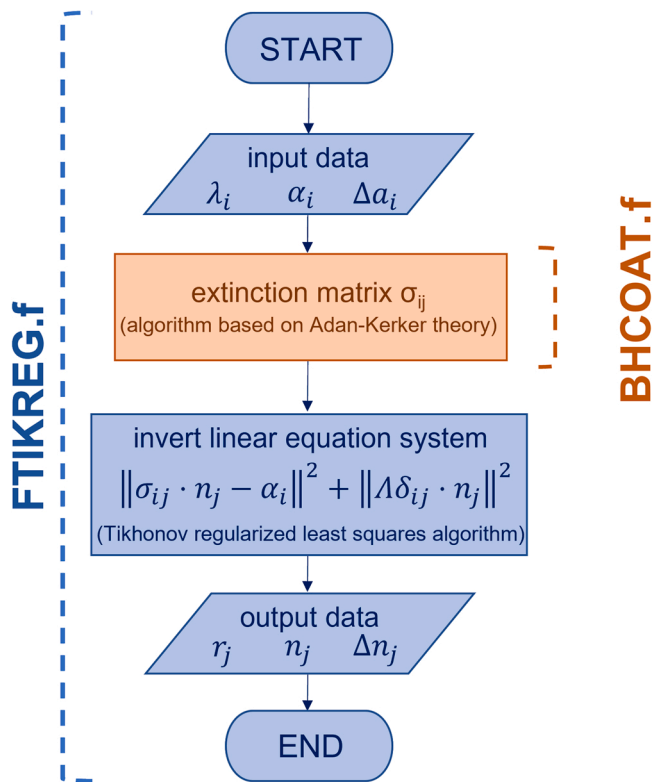

Fig. 2. LTS.f code flow chart. Blue blocks refer to the FTIKREG.f main program that inverts the linear equation system though a Tikhonov regularized least squares algorithm. Orange block indicates the BHCOAT.f subroutine that calculates the extinction matrix for shelled spheres.

4. Results of the LTS experiment

The extinction coefficients and the particle density distribution three selected samples of Soy-PC:Chol 80:20 liposomes at different concentration is shown in Fig. 3. As expected, the amplitude of the extinction coefficients decreases with decreasing lipid amount, and so does the density particle distribution, too.

Fig. 4 shows the complete set of results for suspensions of liposomes obtained by diluting the mother suspension at higher concentration, to cover the typical concentration range used for investigating these nanocarriers. Panel A shows the total particle number concentration of each sample, as a function of the total lipid concentration used in the preparation. The linear dependence of the total particle number concentration on the lipid concentration shown in panel A demonstrates the linearity of the technique (slope $= 1.78 \pm 0.08 \cdot 10^{13}$ part/ml, intercept constrained to zero, 95% confidence level). In panel B, the average radius determined by LTS and DLS is shown. First, the invariance of the LTS radius over the whole concentration range further enforces the LTS method. Comparison of LTS radius with the DLS hydrodynamic radius obtained from cumulant analysis is consistent. As expected, the LTS radius is smaller than the hydrodynamic radius, the difference being ascribable to the DLS overestimation of the contribution of the scattering larger particles in the intensity-weighted physical quantities.

Panel C of Fig. 4 shows a comparison between the lipid mass determined by HPLC and estimated by LTS. First, HPLC has been used to quantify the total lipid concentration of liposomal samples present at the
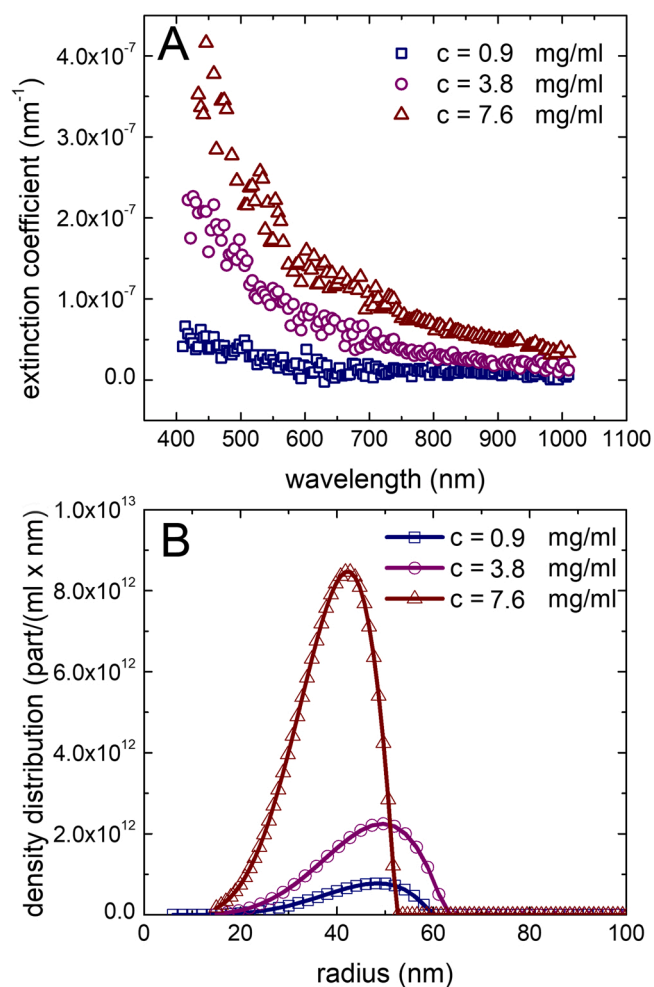
Fig. 3. Extinction coefficient measured by LTS apparatus for Soy-PC:Chol 80:20 liposomes at different concentrations (A), and corresponding particle density distributions obtained by LTS analysis software (B).
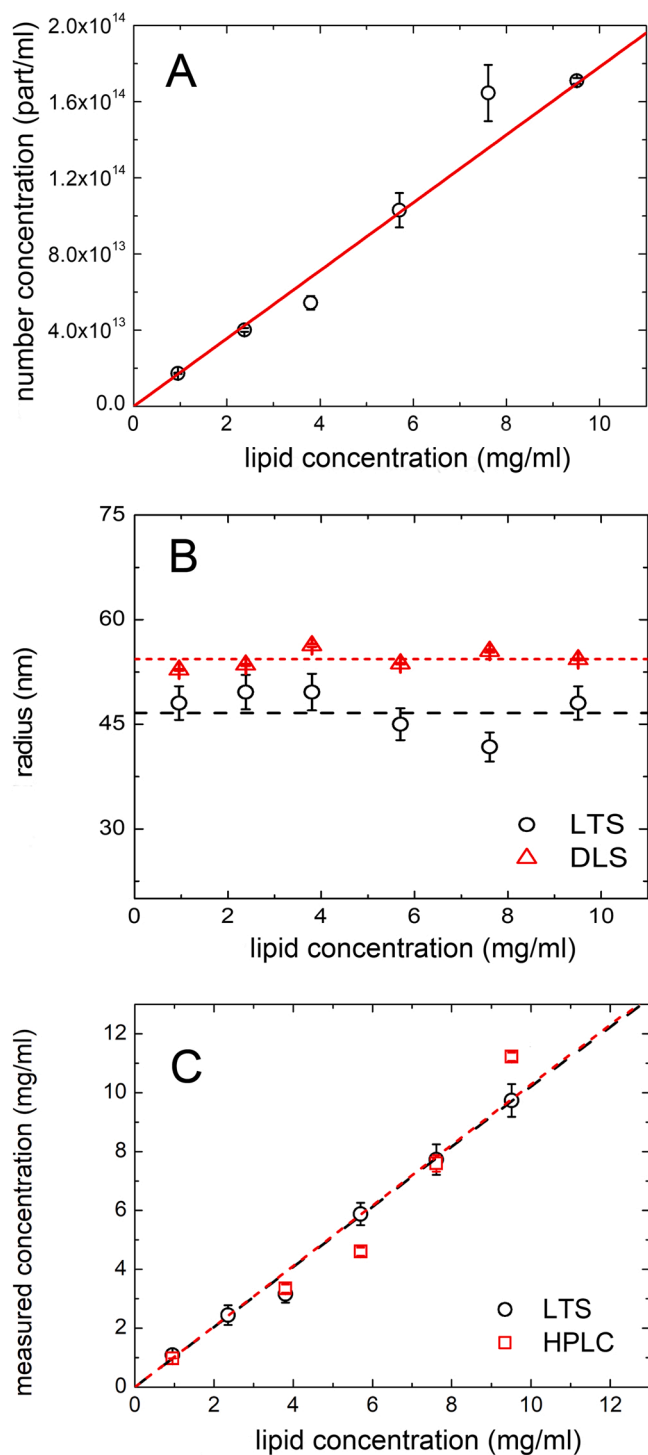
Fig. 4. Total particle number concentration obtained by LTS for Soy-PC:Chol 80:20 liposomes (panel A), corresponding radius evaluated by LTS and DLS (panel B, circles and triangles, respectively), and comparison between the total lipid concentration measured by HPLC technique and calculated by LTS, as a function of the lipid concentration used in the preparation (panel C). Error bars represent the propagated errors for data of panel A and B, and the relative error of 6% in panel C. Dashed lines in panel B and C are the linear fits (B: LTS radius: 47 ± 4; 95% LTS; DLS radius: 54 ± 1; 95%, C: LTS slope: 1.02 ± 0.02 LTS; HPLC slope: 1.03 ± 0.02.).

end of preparation (see SI). The unitary slope of the linear fit of the HPLC-measured concentration in dependence on the lipid concentration used in the preparation (panel C) indicates the absence of lipid loss and full lipid structuring. The LTS total particle number concentration (part/ml) has been converted into mass concentration of lipids (mg/ml) by a geometrical model [34] (see SI for description) and compared with the HPLC quantification. The calculated LTS mass data show a unitary slope and agree with HPLC determination, thus corroborating the validity of LTS analysis. Note that for high concentrations, LTS-derived lipid concentration has a closer correspondence with the nominal values with respect to HPLC. This suggests the use of LTS technique for the estimation of final lipid concentration also in liposomal formulations where HPLC assay is less or not practicable at all.

We showed that LTS technique can be applied to any liposomal formulation, independently of its composition. Fig. 5 reports LTS measurements on HSPC:DPPG liposomes with 6:1 molar ratio at different concentration, loaded with the hydrophilic antitubercolar drug Isoniazid inside the vesicle. As shown for Soy-PC:Chol liposomes, LTS particle number linearly decreases with lipid concentration. As expected, liposomes radius determined by LTS is independent on concentration and lower than the hydrodynamic size. Once again, this supports the validity of this technique to analyse liposomal nanocarriers. It has to be mentioned that LTS measurements have been proven of primary importance in the determination of the total particle number and inner volume of the vesicles which allowed to quantify the drug entrapment capability of INH-loaded HSPC:DPPG liposomes, and evidence the occurrence of drug accumulation at the bilayer due to lipid-drug interaction [19].

5. Future developments

Improvement of the set-up frequency range down to 210 nm to allow measurements of size down to 10 nm is ongoing, as well as the variable gain calibration procedure protocol. This will offer significant advantages also in the investigation of low concentration suspensions of natural vesicles. At the same time, to allow the real-time particle sizing in samples where aggregation or dynamical processes occur, a new set up for Real-Time Light Transmission Spectroscopy is under construction. This set up, with an innovative light source and detection systems, represents a potential improvement respect to other systems already developed [15]. To extend data analysis to objects with other shapes and structures, it is under evaluation the discrete-dipole approximation based routine DDSCATT.f , which allows the calculation of the extinction matrix for any geometry [35,36].

CRediT authorship contribution statement

Simona Sennato: Conceptualization, Validation, Formal analysis, Investigation, Methodology, Project administration, Supervision, Visualization, Writing – original draft, Writing - review & editing. **Angelo Sarra**: Conceptualization, Validation, Data curation, Formal analysis, Investigation, Methodology, Software, Visualization, Writing – original draft, Writing – review & editing. **Carlo Panella La Capria**: Investigation. **Cecilia Bombelli**: Conceptualization, Validation, Investigation, Methodology, Resources, Writing – original draft, Writing – review & editing. **Enrica Donati**: Formal analysis, Investigation, Methodology, Resources, Writing – original draft, Writing - review & editing. **Paolo Postorino**: Project administration, Resources, Software, Supervision, Writing – review & editing. **Federico Bordi**: Project administration, Resources, Software, Supervision, Writing – review & editing.

Declaration of Competing Interest

The authors declare that they have no known competing financial interests or personal relationships that could have appeared to influence the work reported in this paper.
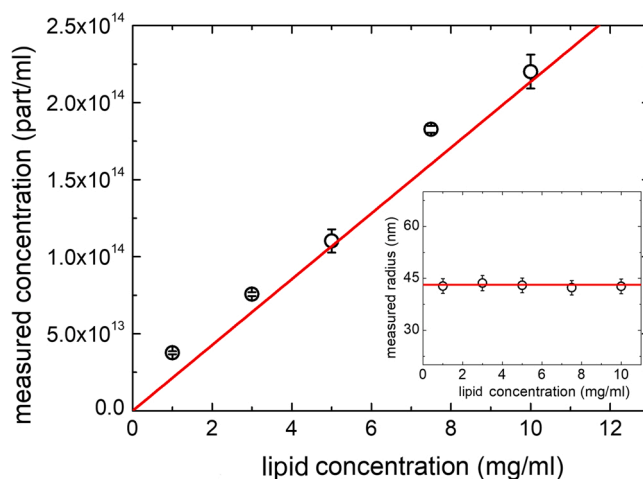

Fig. 5. LTS particle number concentration for HSPC:DPPG 6:1 liposomes loaded with INH drug, and corresponding LTS radius (inset).

Data Availability

Data will be made available on request.

Appendix A. Supporting information

Supplementary data associated with this article can be found in the online version at doi:10.1016/j.colsurfb.2023.113137.

References

[1] P.C. Soema, G.-J. Willems, W. Jiskoot, J.-P. Amorij, G.F. Kersten, Predicting the influence of liposomal lipid composition on liposome size, zeta potential and liposome-induced dendritic cell maturation using a design of experiments approach, Eur. J. Pharm. Biopharm. 94 (2015) 427–435.

[2] Y. Fan, M. Marioli, K. Zhang, Analytical characterization of liposomes and other lipid nanoparticles for drug delivery, J. Pharm. Biomed. Anal. 192 (2021), 113642.

[3] Food and Drug Administration (FDA), Drug products, including biological products, that contain nanomaterials: guidance for industry, 2017 (FDA-2017-D-0759).

[4] P.J. Wyatt, M.J. Weida, Method and apparatus for determining absolute number densities of particles in suspension, 2004.US Patent 6,774,994.

[5] J. Shang, X. Gao, Nanoparticle counting: towards accurate determination of the molar concentration, Chem. Soc. Rev. 43 (2014) 7267–7278.

[6] C.F. Bohren, D.R. Huffman, Absorption and Scattering of Light by Small Particles, John Wiley & Sons, 2008.

[7] J. Irache, C. Durrer, G. Ponchel, D. Duchène, Determination of particle concentration in latexes by turbidimetry, Int. J. Pharm. 90 (1993) R9–R12.

[8] B.J. Berne, R. Pecora, Dynamic light scattering: with applications to chemistry, biology, and physics, Courier Corporation, 2000.

[9] D. Kozak, W. Anderson, R. Vogel, M. Trau, Advances in resistive pulse sensors: devices bridging the void between molecular and microscopic detection, Nano Today 6 (2011) 531–545.

[10] G. Willmott, R. Vogel, S. Yu, L. Groenewegen, G. Roberts, D. Kozak, W. Anderson, M. Trau, Use of tunable nanopore blockade rates to investigate colloidal dispersions, J. Phys. Condens. Matter 22 (2010), 454116.

[11] F. Li, R. Schafer, C.-T. Hwang, C.E. Tanner, S.T. Ruggiero, High-precision sizing of nanoparticles by laser transmission spectroscopy, Appl. Opt. 49 (2010) 6602–6611.

[12] F. Li, A.R. Mahon, M.A. Barnes, J. Feder, D.M. Lodge, C.-T. Hwang, R. Schafer, S. T. Ruggiero, C.E. Tanner, Quantitative and rapid DNA detection by laser transmission spectroscopy, PLoS One 6 (2011), e29224.

[13] A.R. Mahon, M. Barnes, F. Li, S.P. Egan, C.E. Tanner, S.T. Ruggiero, J.L. Feder, D. M. Lodge, DNA-based species detection capabilities using laser transmission spectroscopy, J. R. Soc. Interface 10 (2013), 20120637.

[14] A. Sarra, G.D.P. Stanchieri, A. De Marcellis, F. Bordi, P. Postorino, E. Palange, Laser transmission spectroscopy based on tunable-gain dual-channel dual-phase LIA for biological nanoparticles characterization, IEEE Trans. Biomed. Circuits Syst. 15 (2021) 177–187.

[15] J. Yoon, S. Park, K.M. Chun, S. Song, Development of a real-time, in-situ particle sizing technique: real-time light transmission spectroscopy (RTLTS), Aerosol Sci. Technol. 47 (2013) 1092–1100.

[16] W.J. Wiscombe, Improved Mie scattering algorithms, Appl. Opt. 19 (1980) 1505–1509.

[17] J. Weese, A reliable and fast method for the solution of Fredholm integral equations of the first kind based on tikhonov regularization, Comput. Phys. Commun. 69 (1992) 99–111.

[18] W.C. Poon, E.R. Weeks, C.P. Royall, On measuring colloidal volume fractions, Soft Matter 8 (2012) 21–30.

[19] F. Sciolla, D. Truzzolillo, E. Chauveau, S. Trabalzini, L. Di Marzio, M. Carafa, C. Marianecci, A. Sarra, F. Bordi, S. Sennato, Influence of drug/lipid interaction on the entrapment efficiency of isoniazid in liposomes for antitubercular therapy: a multi-faced investigation, Colloids Surf. B: Biointerfaces 208 (2021), 112054.

[20] A. Grimaldi, C. Serpe, G. Chece, V. Nigro, A. Sarra, B. Ruzicka, M. Relucenti, G. Familiari, G. Ruocco, G.R. Pascucci, et al., Microglia-derived microvesicles affect microglia phenotype in glioma, Front. Cell. Neurosci. 13 (2019) 41.

[21] M. De Robertis, A. Sarra, V. D'Oria, F. Mura, F. Bordi, P. Postorino, D. Fratantonio, Blueberry-derived exosome-like nanoparticles counter the response to TNF-α-induced change on gene expression in EA.hy926 cells, Biomolecules 10 (2020) 742.

[22] H. Epstein, E. Afergan, T. Moise, Y. Richter, Y. Rudich, G. Golomb, Number-concentration of nanoparticles in liposomal and polymeric multiparticulate preparations: empirical and calculation methods, Biomaterials 27 (2006) 651–659.

[23] M. Hope, R. Nayar, L. Mayer, P. Cullis, Liposome technology, 1993.

[24] R. MacDonald, R. MacDonald, Applications of freezing and thawing in liposome technology, Liposome Technol. 1 (1993) 209–228.

[25] X. Xu, M.A. Khan, D.J. Burgess, Predicting hydrophilic drug encapsulation inside unilamellar liposomes, Int. J. Pharm. 423 (2012) 410–418.

[26] N. Nguyen, A note on Tikhonov regularization of linear ill-posed problems, Mass. Inst. Technol. (2006) 1–4.

[27] A.N. Tikhonov, V.I. Arsenin, Solutions of ill-posed problems, Wiley, 1977.

[28] J. Weese, A reliable and fast method for the solution of Fredholm integral equations of the first kind based on Tikhonov regularization, Comput. Phys. Commun. 69 (1992) 99–111.

[29] J. Weese, FTIKREG: A program for the solution of Fredholm integral equations of the first kind, user manual, 1991.

[30] G.M. Hale, M.R. Querry, Optical constants of water in the 200-nm to 200-μm wavelength region, Appl. Opt. 12 (1973) 555–563.

[31] N. Sultanova, S. Kasarova, I. Nikolov, Dispersion properties of optical polymers, Acta Phys. Pol. -Ser. A Gen. Phys. 116 (2009) 585.

[32] P.B. Johnson, R.-W. Christy, Optical constants of the noble metals, Phys. Rev. B 6 (1972) 4370.

[33] I.H. Malitson, Interspecimen comparison of the refractive index of fused silica, Josa 55 (1965) 1205–1209.

[34] J. Montanari, P. Bucci, S. d.V. Alonso, A model based in the radius of vesicles to predict the number of unilamellar liposomes, Int. J. Res. Pharm. Chem. 4 (2014) 484–489.

[35] B.T. Draine, P.J. Flatau, Discrete-dipole approximation for scattering calculations, J. Opt. Soc. Am. A 11 (1994) 1491–1499.

[36] B.T. Draine, P.J. Flatau, Discrete-dipole approximation for periodic targets: theory and tests, J. Opt. Soc. Am. A 25 (2008) 2693–2703.